https://dx.doi.org/10.1016/j.matdes.2017.01.052

Quantification of bituminous mortar ageing and its application in ravelling evaluation of porous asphalt wearing courses

Yuan Zhang, Zhen Leng*

Department of Civil and Environmental Engineering, The Hong Kong Polytechnic University, Hung Hom, Kowloon, Hong Kong

*Corresponding author. Tel.: +852 2766 6007; Fax: +852 2334 6389. E-mail address: zhen.leng@polyu.edu.hk.

Abstract: Bituminous mortar, consisting of bitumen, filler and fine aggregates (<0.5 mm), plays a dominating role on the viscoelastic properties of Porous Asphalt (PA), and its ageing is one of the key factors causing the ravelling of PA wearing courses. This research is to quantify the ageing effect on the rheological characteristics of bituminous mortars and apply it in evaluation of the ravelling resistance of PA wearing courses. Bituminous mortars for two types of PA (one with base bitumen and the other with Styrene-Butadiene-Styrene (SBS) modified bitumen) were artificially aged in the laboratory. Cylindrical specimens were then prepared with the aged mortars and their complex shear modulus and shear fatigue life were characterized through the Dynamic Shear Rheometer (DSR) tests. Finite element models containing the structural geometries and material responses of the two PA wearing courses were created. Their stresses and strains under traffic loads were simulated and analysed. The experimental results showed that ageing had more influence on the complex shear modulus of the base mortar compared to the SBS mortar. However, its effects on fatigue resistance are opposite. The numerical modelling results indicated that after ageing, the ravelling resistance of the PA wearing course with base mortar decreased more.

Keywords: Porous asphalt; Bituminous mortar; Ageing; Dynamic shear rheometer; Finite element modelling

1. Introduction

Due to its extremely high population density, Hong Kong has shown increasing interests in low-noise road surfacing (LNRS) materials, such as Porous Asphalt (PA). PA is an open-graded asphalt mixture composed of aggregate skeleton, bituminous mortar and high percentage of air voids. Because of the high air void content (>20%), PA wearing courses have excellent performance in rolling noise reduction. Both base bitumen without polymer modification and polymer modified bitumen have been used to build PA wearing courses in Hong Kong. But the PA with polymer modified bitumen was found more cost-effective because of its higher durability, and has been used as the standard surfacing material in highways in force since 2007 [1].

Japan, which decided to use PA for all highways as a standard surface material, has long-term experience with PA wearing courses. The Japan experience has shown that PA with conventional polymer modified bitumen containing 5% Styrene-Butadiene-Styrene (SBS) has poor durability. It was found that a special polymer modified bitumen containing 9% SBS extended the service life of the PA wearing courses, and has been used in force since 1998 [2, 3]. Within the United States, Georgia Department of Transportation (DOT) developed the specification for the first generation of PA in the 1990s. After that a number of states in the southern part of the Unities State specified PA and utilized it as the wearing course on all interstates. Most agencies specified polymer modified bitumen. Researches and field applications indicate that polymer modified bitumen, together with stabilizing fibre, can extend the service life and eliminate the ravelling problems [4-7]. The Netherlands, which has PA wearing courses on more than 90% of its main highway network, also has long-term experience with PA wearing courses. But contradictory to the experience in Hong Kong and many other regions, the Dutch experience has shown that polymer modified bitumen has no effect on the service life extension of PA wearing courses. It was reported that polymer modified bitumen was only useful to obtain a higher binder content in PA which led to a better behaviour in the field, but the same improvement could be obtained with base bitumen and drainage inhibitor [8-13]. These oversea experiences can lead to different polices for the design of PA wearing courses at large scaled application. Thus, it is worth to study and understand the benefits of using base and polymer modified bitumen in PA to improve the design of PA wearing courses in Hong Kong.

Bituminous mortar, also commonly known as fine aggregate matrix in North America, consists of bitumen, filler and fine aggregates smaller than the minimum aggregate size in the aggregate skeleton. It plays a dominating role on the viscoelastic properties of PA. Various studies have shown the potential of testing bituminous mortar as an efficient and repeatable approach to predict the performance of asphalt mixture. For instance, Mohammad et al. [12, 13] investigated the viscoelastic behaviour of the bituminous mortar and hot mix asphalt. Certain linkages between them were found and used to explain the effect of hydrated lime under moisture damage conditions. Huurman et al. [14-17] designed a mechanistic lifetime optimization tool for PA, based on the experimental tests of the behaviour of bituminous mortar and the adhesive bond between stone and bituminous mortar. It was found that the lifetime optimization tool calculations had a strong correlation with the full-scale PA performance. Underwood and Kim [18] found that bituminous mortar can be useful for both practical and model tasks with proper material design and testing. Sousa et al. [19] developed a new procedure for preparing bituminous mortar specimens and conducted fracture mechanics-based analysis of damage in bituminous mortar. He et al. [20] reported that the bituminous mortar testing can be considered as an effective alternative approach to chemical binder extraction for characterizing the properties of blended binders in asphalt mixtures containing high quantities of reclaimed asphalt pavement.

The high air void content makes PA more sensitive to damage due to traffic and environmental effects than dense-graded mixtures. Ravelling, defined as the loss of stone particles from the pavement surface, is the most common type of damage of PA. Due to ravelling, the average service life of PA wearing courses is usually shorter than that of dense-graded wearing courses [8-10]. Ageing of bituminous binder is believed to be one of the main reasons for ravelling damage of PA wearing courses [21, 22]. Therefore, the benefits of using base and polymer modified bitumen in PA can be investigated through quantification of bituminous mortar ageing and evaluation of ravelling resistance of PA wearing courses with aged mortars.

The main objectives of this study are to quantify the ageing effect on the rheological characteristics of bituminous mortars and apply it in evaluation of the ravelling resistance of PA wearing courses. To achieve these objectives, bituminous mortars for two typical types of PA wearing courses, one with base bitumen and the other with SBS modified bitumen, were artificially aged in the laboratory. Cylindrical specimens were then prepared with these aged mortars and tested using the Dynamic Shear Rheometer (DSR). Their rheological properties were characterized by constructing the master curves of complex shear modulus and phase angle, and determining the shear fatigue lives at various shear strain levels, respectively. Finite element models containing the structural geometries and material responses of the two PA wearing courses were created in the program ABAQUS. The stresses and strains in these two PA wearing courses under traffic loads were simulated and analysed.

2. Experimental Programs and Numerical Models

2.1 Materials

Bituminous mortars for two types of PA were studied in this research. One is the PA 0/16, which has been widely used as highway surfacing material in the Netherlands. It consists of crushed stones with a nominal maximum aggregate size of 16 mm, crushed sand, mineral filler and base bitumen with a penetration grade of 70/100. Its bitumen content is 5.5% by mass of total mineral aggregates [9]. The other is the PA 0/10, which is the typical type of PA used in Hong Kong. This mixture consists of crushed stones with a nominal maximum aggregate size of 10 mm, crushed sand, mineral filler and SBS modified bitumen with a Superpave performance grade of PG76. It has a bitumen content of 5.8% by mass of total mineral aggregates [1]. The gradations of these two asphalt mixtures are presented in Table 1. The gradations of PA 0/16 and PA 0/10 were used to calculate the material compositions of their bituminous mortars.

Table 1: Gradations of the asphalt mixtures PA 0/16 and PA 0/10.

Mixture	Sieve size (mm)	22.4	16.0	11.2	8.0	5.6	2.0	0.5	0.18	0.063
PA 0/16	Passing percentage	100	97.0	73.0	47.0	22.0	15.0	9.3	6.0	4.5
PA 0/10	Passing percentage	100	100	97.0	65.0	21.0	14.0	8.0	5.8	4.2

According to Muraya's research on aggregate skeletons of asphalt mixtures [23], the aggregate skeleton in PA is composed of aggregates with sizes larger than 0.5 mm. Therefore, the bituminous mortar used in this research contained fine aggregates with sizes smaller than 0.5 mm. In order to determine binder content of the bituminous mortar, it was assumed that all mineral aggregates in PA mixture are coated with a thin bitumen film of 10 μm [14, 15]. The binder content of bituminous mortars was calculated by deducting the amount of bitumen that coats the aggregates with sizes larger than 0.5 mm from the total amount of bitumen used in the asphalt mixture. The surfaces of aggregates were estimated by simplifying the aggregates as spheres with representative sizes. Table 2 presents the material compositions of the two bituminous mortars used in this research.

Table 2: Material compositions of the bituminous mortars.

Mortar type	Mixture	Fine aggregates (0.5-0.063 mm)	Mineral filler (<0.063 mm)	Binder
Mortar with base bitumen	PA 0/16	33%	31%	36%
Mortar with SBS modified bitumen	PA 0/10	27%	33%	40%

To prepare bituminous mortar, fine aggregates, mineral filler and bitumen were completely mixed at a temperature of 165 ^{o}C. Afterwards, the bituminous mortar was aged in an oven at 165 ^{o}C for 2 hours and then in a Pressure Ageing Vessel (PAV) at 100 ^{o}C for 80 hours under an air pressure of 2.1 MPa. During the ageing process, 50 gram of bituminous mortar was placed on a steel plate with a diameter of 140 mm.

Cylindrical mortar specimens for testing were prepared with both the fresh and aged bituminous mortars. A picture of the cylindrical mortar specimens and the schematic diagram of its geometry are given in Figure 1 (a) and (b), respectively. The total height of the cylindrical mortar specimen is 20 mm. At both ends, the cylindrical mortar specimen is enclosed by a steel block to allow clamping it into the measuring system of DSR. Over the central 10 mm length, the cylindrical mortar specimen has a constant diameter of 6 mm.

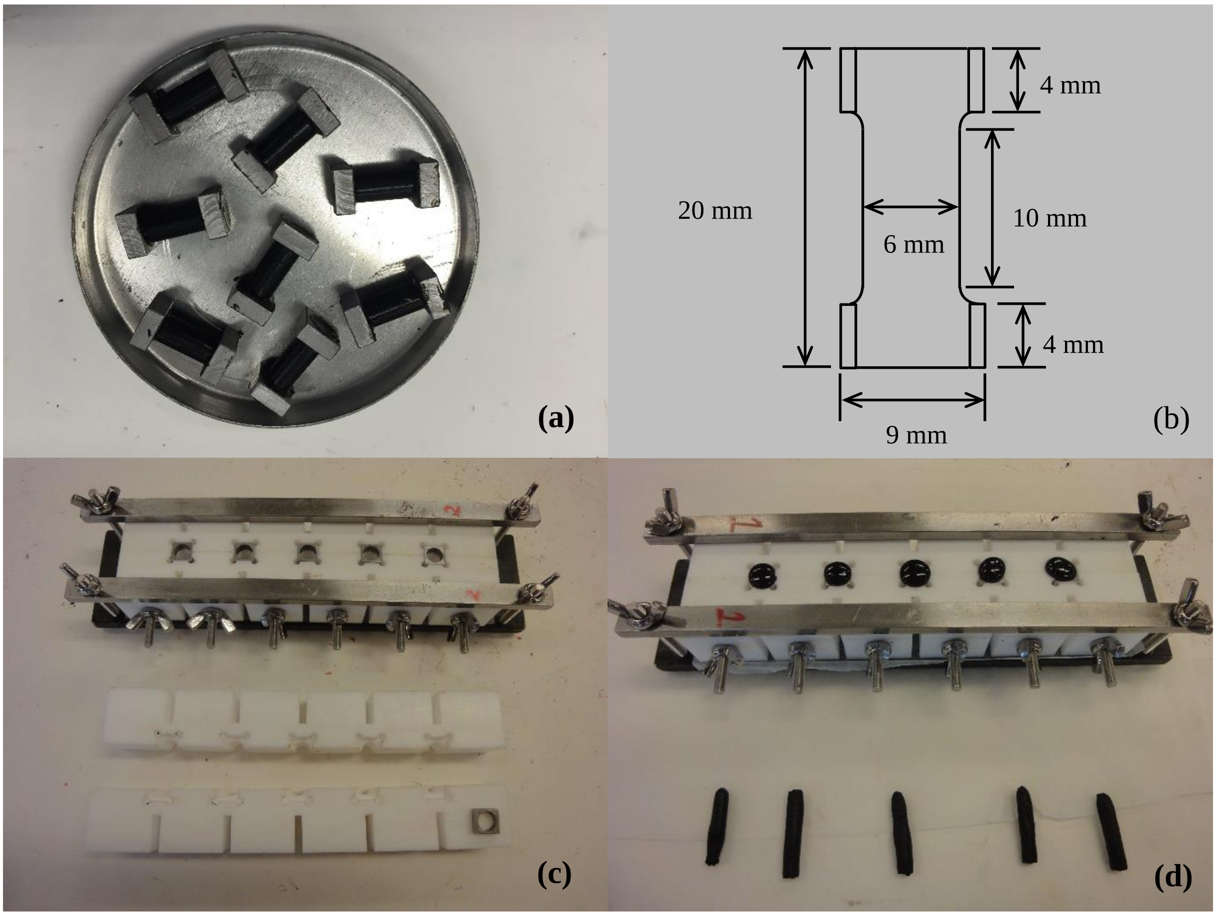

Figure 1: Bituminous mortar specimens and the mould for preparation: (a) cylindrical mortar specimens; (b) schematic diagram of specimen geometry; (c) Teflon mould; (d) filling mortar into the mould.

A specially designed Teflon mould as shown in Figure 1 (c) was used to prepare the cylindrical mortar specimens. The bituminous mortar was first cooled down on silicon paper at room temperature. During the cooling process, the bituminous mortar was shaped into cylinders with a diameter of around 6 mm (see Figure 1 (d)). After heating the Teflon mould up to a temperature of 165 ^{o}C in an oven, these cylinders were inserted into the pre-heated Teflon mould and kept in the oven for 10 minutes. Then they were taken out from the oven and cooled down at room temperature. In order to remove the cylinder mortar specimens from the Teflon mould, they were stored in a fridge at a temperature of -10 ^{o}C for 2 hours. Then the Teflon mould was split by releasing the screws, after which the specimens could be removed without any damage. Before testing, all the cylindrical mortar specimens were stored in a fridge at a temperature of 5 ^{o}C to avoid development of any deformation.

2.2 Test methods

The dynamic shear tests for measuring the rheological properties of the cylindrical mortar specimens were performed with the DSR MCR702. A special feature of this DSR equipment is that it can perform rheological tests with one drive unit for applying loading at bottom and another drive unit for recoding response at top simultaneously, which delivers more precise results. A special measuring system designed for solid specimen was used to mount the cylindrical mortar specimens in the DSR (see Figure 2 (b)).

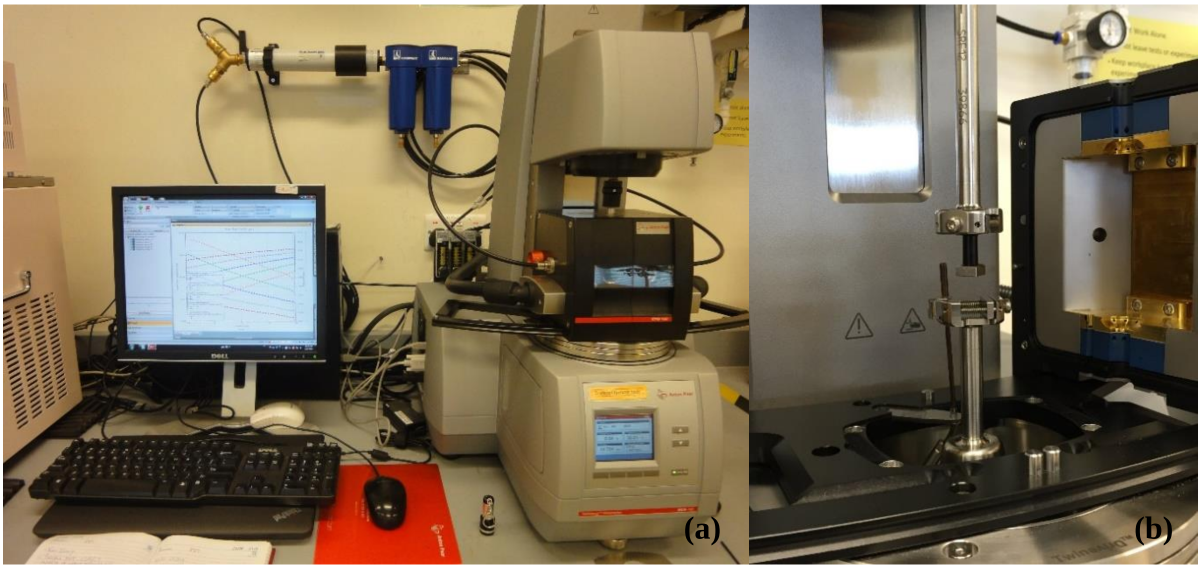

Figure 2: Dynamic shear test devices: (a) front view of DSR MCR702; (b) measuring system for solid specimens.

The dynamic shear tests were conducted in the strain-controlled mode. In the tests, a sinusoidal deformation at a certain shear strain level was applied to the testing specimen. The applied deformation and the corresponding torque were measured and the phase lag between these two signals was determined. For the measurement of complex shear modulus, frequency sweep tests from 100 to 0.01 Hz were performed on five mortar specimens at the test temperatures of -10, 0, 10, 20 and 30 ^{o}C, respectively. In order to determine the strain level at which the mortar behaves linearly, a strain amplitude sweep test at each test temperature was carried out in advance. For the measurement of shear fatigue life, a continuous oscillating deformation was applied to each test specimen until it was broken. Various strain levels, which were high enough to develop fatigue damage, were chosen for different types of bituminous mortar in shear fatigue tests. For each type of bituminous mortar, shear fatigue tests were performed on nine specimens at 10 ^{o}C and 10 Hz.

2.3 Finite element models

From the high-resolution Computed Tomography (CT) scanning image of PA, its three components (i.e. aggregate skeleton, bituminous mortar and air voids) can be discriminated clearly (see Figure 3 (b) and (d)). Two-dimensional finite element models allowing the real structure of the PA to be simulated, were created in the program ABAQUS, based on the high-resolution CT scanning images of PA 0/16 and PA 0/10. The method of creating the finite element models has been reported in previous studies [24, 25]. The PA 0/16 and PA 0/10 models used in this research (see Figure 3 (a) and (c)), have dimensions of 150 mm in length and 25 mm in height.

In the finite element models, the stone particles which have much higher stiffness than bituminous mortars, were simulated as rigid bodies in order to limit the mathematical size of the models. The material response of bituminous mortars was a time domain viscoelastic material mode that is built in ABAQUS by means of Prony series. The terms in Prony series were calibrated using the frequency-dependent master curve data from DSR tests [25, 26]. In Hagos's research on the effect of ageing on binder properties on PA [21], it was concluded that ageing is the main reason for ravelling failure in PA wearing course because of its effects on the cohesive characteristic of the binding material. So in the finite element modelling of this research the stone particles were tied together with the bituminous mortars. The adhesive behaviour between mortar and stone was not investigated.

The load signals applied in models were derived from actually occurring contact stresses between tire and pavement surface. The program TyreStress [27] was used to simulate the tire contact stresses. A 425/65 R22.5 tire with a load of 50 kN and a tire inflation pressure of 0.8 MPa was used to generate the tire contact stress distributions. Then the vertical and longitudinal stress signals as a function of time were obtained for the wheel load travelling at a speed of 80 km/h. Afterwards, the stress signals were transformed into force signals that can be applied on the stone particles at the surface of the models. The method of acquiring the load signals and the load signals themselves can be found in a former research [25].

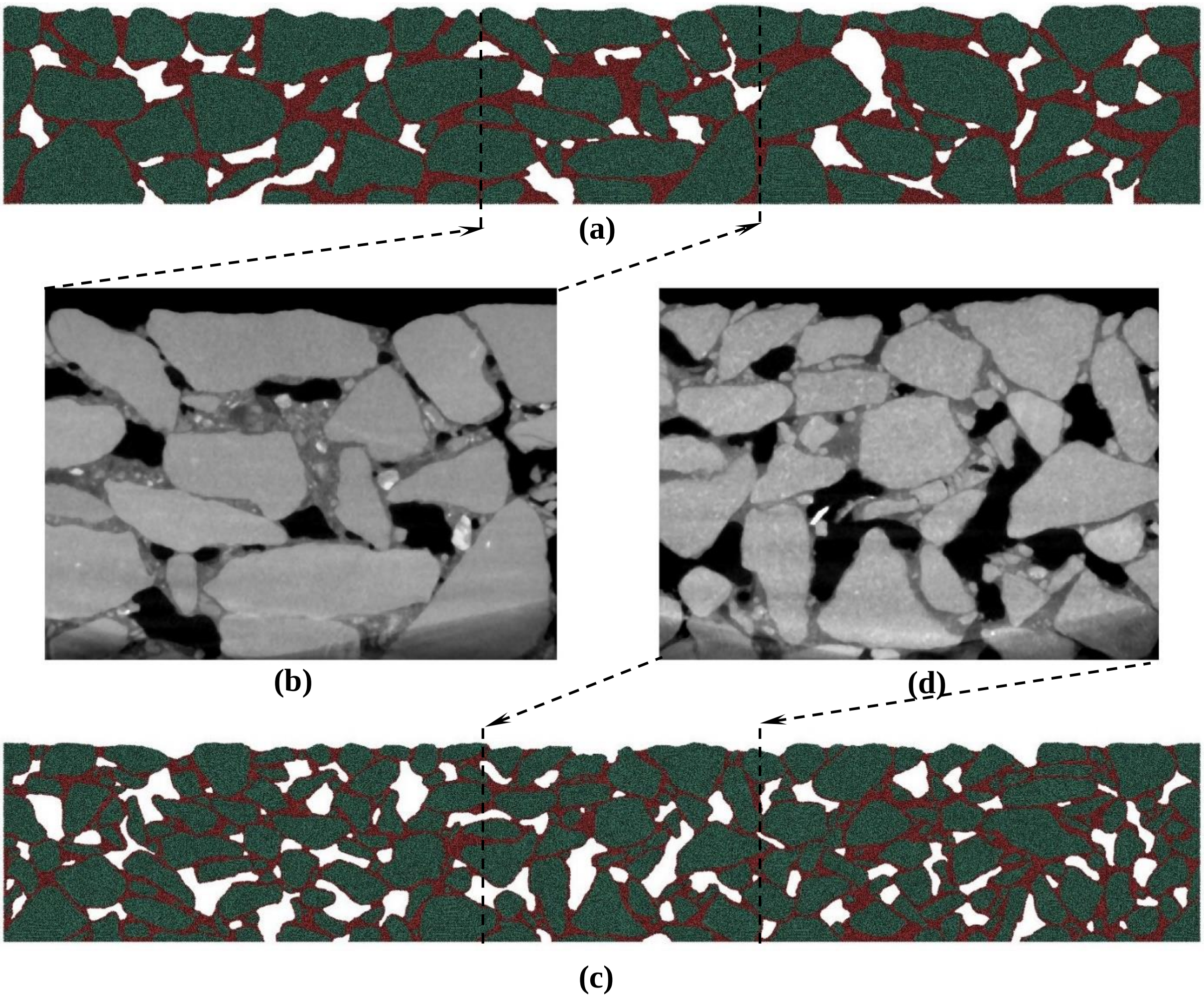

Figure 3: Structural models and CT scanning images for PA wearing courses: (a) and (b) for PA 0/16; (c) and (d) for PA 0/10.

3. Results and Discussion

3.1 Chemical properties of reclaimed bituminous binders

In order to determine laboratory ageing level, the chemical properties of reclaimed bituminous binders from the laboratory-aged mortars were compared with those of reclaimed bituminous binders from field-aged asphalt mixtures. The field-aged asphalt mixtures were obtained from two PA wearing courses which were both approximately 5 years old [9, 28]. The bituminous binders used in those two PA wearing courses were base bitumen and SBS modified bitumen, respectively. They had similar engineering properties as the bituminous binders used for preparing the mortars in this research, although they were from different sources. In this paper, the reclaimed bituminous binders from the laboratory-aged mortars with base bitumen and SBS modified bitumen are referred to as aged base bitumen @ lab and aged modified bitumen @ lab, respectively. The reclaimed bituminous binders from the field-aged asphalt mixtures with base bitumen and SBS modified bitumen are referred to as aged base bitumen @ field and aged modified bitumen @ field, respectively.

Ageing of bituminous binders is mainly caused by oxidation. The presence of oxidation groups are therefore important factors for detecting ageing in infrared spectra. The oxidation groups for bituminous binders, namely ketones (C=O) at the wavenumber of 1700 cm^{-1} and sulfoxides (S=O) at the wavenumber of 1030 cm^{-1}, are two important ageing indicators. Figure 4 illustrates the representative infrared spectra of the reclaimed bituminous binders at a wavenumber region of 1800-600 cm^{-1}. The specific absorption peaks at the wavenumber of around 1700 cm^{-1} are observed in the infrared spectra of all aged bituminous binders, but not in those of the fresh bituminous binders. The specific absorption peaks at the wavenumber of around 1030 cm^{-1} in the infrared spectra of all aged bituminous binders are larger than those of the fresh bituminous binders.

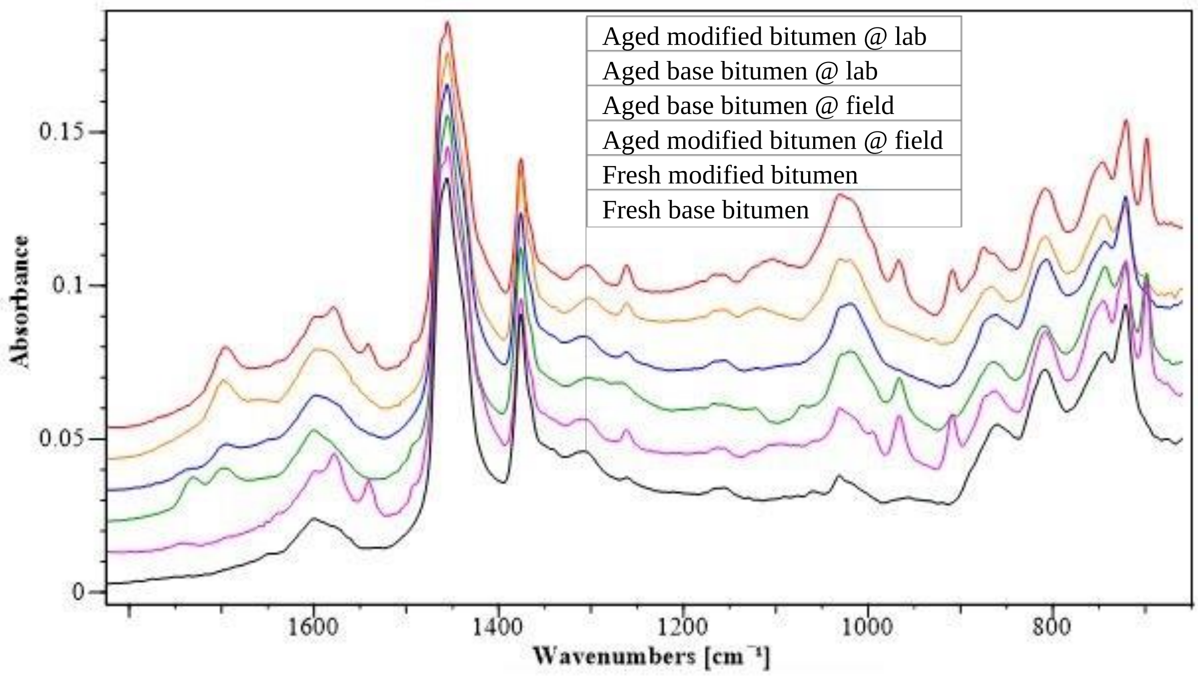

Figure 4: Representative infrared spectra of the reclaimed bituminous binders.

From the infrared spectra, the semi-quantitative method proposed by Lamontagne et al. [29] was used to determine the ageing levels of the reclaimed bituminous binders. In this semi-quantitative method, the sum of the areas at some specific bands is believed not to be influenced by ageing and therefore can be used as a reference. Areas of the specific bands are compared with this reference. Several structural and functional indices can be calculated from the band areas using Equations 1 to 6:

$$Aromaticity\ index = \frac{A_{1600}}{\sum A} \tag{1}$$

$$Aliphatic\ index = \frac{A_{1460} + A_{1376}}{\sum A} \tag{2}$$

$$Branched\ aliphatic = \frac{A_{1376}}{A_{1460} + A_{1376}} \tag{3}$$

$$Long\ chains = \frac{A_{724}}{A_{1460} + A_{1376}} \tag{4}$$

$$Carbonyl\ index = \frac{A_{1700}}{\sum A} \tag{5}$$

$$Sulfoxide\ index = \frac{A_{1030}}{\sum A} \tag{6}$$

Where A_{xxx} represents the area at a specific band of spectrum; ΣA is the summation of areas from $A_{(2953,\ 2923,\ 2862)}$; A_{1700}, A_{1600}, A_{1460}, A_{1376}, A_{1030}, A_{864}, A_{814}, A_{743} and A_{724}.

The carbonyl index and sulfoxide index are functional indices representing the rate of oxidation groups in the bituminous binders, while others are structural indices. Table 3 presents the structural and functional indices of the reclaimed bituminous binders.

Table 3: Structural and functional indices of the reclaimed bituminous binders.

Material	Aromatici-ty index	Aliphatic index	Branched aliphatic	Long chains	Carbonyl index	Sulfoxide index
Fresh base bitumen	0.052	0.275	0.174	0.037	0.000	0.021
Aged base bitumen @ lab	0.058	0.264	0.179	0.039	0.018	0.032
Aged base bitumen @ field	0.048	0.250	0.152	0.059	0.017	0.031
Fresh modified bitumen	0.069	0.261	0.142	0.072	0.000	0.021
Aged modified bitumen @ lab	0.063	0.248	0.149	0.074	0.017	0.038
Aged modified bitumen @ field	0.045	0.255	0.158	0.035	0.020	0.031

Compared with the fresh base bitumen, the aged base bitumen @ lab showed significant higher carbonyl and sulfoxide indices, while the structural indices did not change obviously. Similar findings were obtained between the aged modified bitumen @ lab and fresh modified bitumen as well. The carbonyl and sulfoxide indices of the aged base bitumen @ lab were close to those of the aged base bitumen @ field. The differences in their structural indices may be due to the difference in binder sources. The aged modified bitumen @ lab also showed similar carbonyl and sulfoxide indices compared with the aged modified bitumen @ field. In other words, the ageing performed on the bituminous mortars in this research simulated approximately 5-year field ageing of PA wearing courses, in terms of the carbonyl and sulfoxide indices of the reclaimed bituminous binders.

In addition, it can be found that the aged base bitumen and aged modified bitumen exhibited very similar carbonyl and sulfoxide indices. This means that after the long-term ageing, the base bitumen and modified bitumen tend to have a similar ageing level.

3.2 Complex shear modulus of bituminous mortars

Master curves of the complex shear modulus and phase angle as a function of the reduced frequency were constructed at a reference temperature of 10 ^{o}C by using the time-temperature superposition principle. The shift factors used to obtain the master curves were determined by means of the Williams-Landel-Ferry (WLF) formula given in Equation 7:

$$\log a_T = \frac{-C_1(T - T_0)}{C_2 + (T - T_0)} \tag{7}$$

Where a_T is shift factor; T is test temperature; T_0 is reference temperature; C_1 and C_2 are constants.

To fit the frequency-dependent master curves, the Modified Huet-Sayegh (MHS) model developed by Woldekidan et al. [16] was chosen in this research. The MHS model is capable of describing the response of bituminous binders as well as mixtures over a wide frequency window. In the MHS model, a linear dashpot is placed in series with the original Huet-Sayegh (HS) model [30]. This improves the low frequency region fitting of the model to the master curve data and also allows the model to simulate viscous deformations. Equation 8 provides the mathematical expression of the MHS model:

$$J^*(\omega) = \frac{G'}{|G^*(\omega)|^2} - i\left[\frac{G''}{|G^*(\omega)|^2} + \frac{1}{\eta_3\omega}\right] = J'(\omega) - iJ''(\omega) \tag{8}$$

Where $J^*(\omega)$ represents the complex creep compliance of the MHS model; G^* is the complex shear modulus of original HS model; G' is the storage shear modulus of original HS model;

G'' is the loss shear modulus of original HS model; η_3 is linear dashpot parameter; $J'(\omega)$ represents the storage creep compliance of the MHS model; and $J''(\omega)$ represents the loss creep compliance of the MHS model.

The expressions for the complex, storage and loss shear modulus of original HS model can be obtained using the following equations [30]:

$$G^*(\omega) = G_0 + \frac{G_\infty - G_0}{1 + \delta_1 (i\omega\tau_1)^{-m_1} + \delta_2 (i\omega\tau_2)^{-m_2}} \tag{9}$$

$$\delta_i = \frac{\tau_{i(G_\infty - G_0)}}{\eta_i} \tag{10}$$

$$G' = G_0 + A \frac{G_\infty - G_0}{A^2 + B^2} \tag{11}$$

$$G'' = B \frac{G_\infty - G_0}{A^2 + B^2} \tag{12}$$

$$A = 1 + \delta_1 \frac{\cos\left(m_1 \frac{\pi}{2}\right)}{(\omega\tau)^{m_1}} + \delta_2 \frac{\cos\left(m_2 \frac{\pi}{2}\right)}{(\omega\tau)^{m_2}} \tag{13}$$

$$B = \delta_1 \frac{\sin\left(m_1 \frac{\pi}{2}\right)}{(\omega\tau)^{m_1}} + \delta_2 \frac{\sin\left(m_2 \frac{\pi}{2}\right)}{(\omega\tau)^{m_2}} \tag{14}$$

Where G_∞ is the instantaneous shear modulus; G_0 is the rubbery shear modulus; δ_1 and δ_2 are model parameters; m_1 and m_2 are the parabolic dashpot coefficients; η_1 and η_2 are parabolic dashpots' parameters; τ_1 and τ_2 are time constants; and A and B are the variables.

The MHS model has a total of nine independent parameters. For response modelling of bituminous materials, only one time constant ($\tau=\tau_1=\tau_2$) is usually used and the model parameter δ_2 is considered as unity [31]. Consequently, only seven parameters are required to describe the complete response of bituminous materials covering various temperature and frequency regions.

For each type of bituminous mortar, the measured complex shear moduli and phase angles of five cylindrical mortar specimens at five test temperatures were shifted to the reference temperature of 10 ^{o}C in order to create master curves. Then the master curve data were fitted by means of the MHS model. The master curves of the complex shear moduli and phase angles of the fresh and aged bituminous mortars are shown in Figure 5. The high anastomosis within test results from five specimens in the master curves implies that the rheological tests of the cylindrical mortar specimens provided very good testing repeatability. As expected, ageing increased the complex shear modulus and decreased the phase angle significantly over a wide frequency range (1.0E-04 to 1.0E+04 Hz), indicating that the aged bituminous mortars became stiffer.

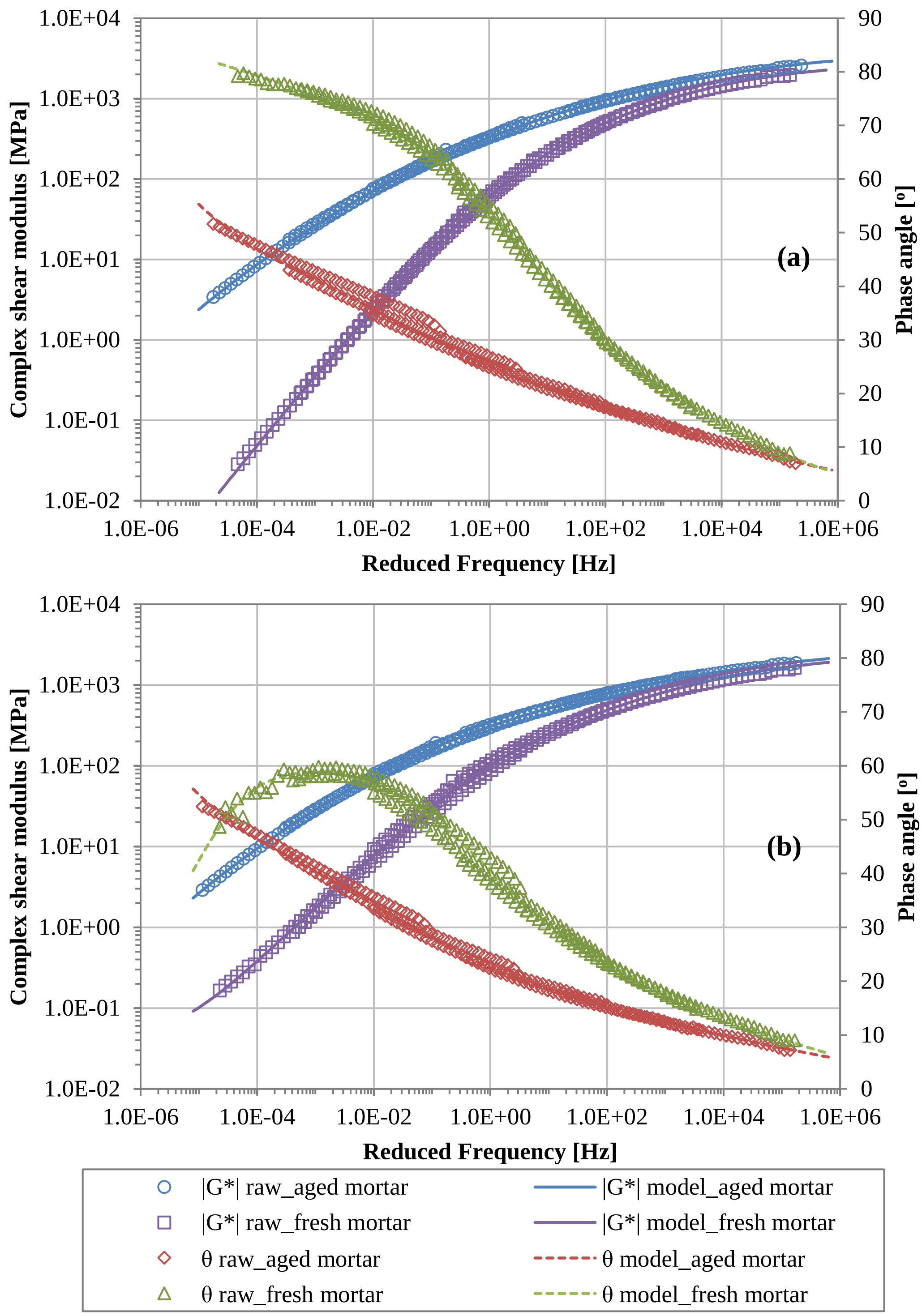

Figure 5: Master curves of the complex shear modulus and phase angle of bituminous mortars at a reference temperature of 10 °C: (a) mortars with base bitumen; (b) mortars with SBS modified bitumen.

The fresh mortar with base bitumen showed lower complex shear moduli and higher phase angles than the fresh mortar with SBS modified bitumen, especially at frequencies lower than

1 Hz. However, after ageing, their complex shear moduli and phase angles were similar at all frequencies. Hence, it can be concluded that ageing had more influence on the complex shear modulus and phase angle of the mortar with base bitumen compared with the mortar with SBS modified bitumen.

For the fresh mortar with SBS modified bitumen, reduction in phase angles at a low frequency range from 1.0E-05 to 1.0E-03 Hz (corresponding to high temperature range) was observed. This phenomenon also occurs in the master curve of phase angle of SBS modified bitumen, which is attributed to the SBS polymers network in binder. However, for the aged mortar with SBS modified bitumen, no such reduction in phase angles was found. The possible reason is that the SBS polymers had degraded after ageing.

Besides, Figure 5 shows that the master curves of complex shear modulus and phase angle for all bituminous mortars are well described by the MHS model. Table 4 presents the model parameters of these master curves. The values of the coefficient of determination (R^2) are all higher than 0.99. This proves the good agreement between the MHS model prediction and the measured data. The model fitted data were used to calibrate the Prony series terms of the bituminous mortars for finite element modelling.

Table 4: Model parameters of the master curves of complex shear modulus and phase angles of the bituminous mortars.

Parameters			Mortar with base bitumen		Mortar with SBS modified bitumen	
			fresh	aged	fresh	aged
WLF formula	C_1	[-]	17.5	29.6	29.7	62.2
	C_2	[-]	130.4	195.2	204.3	403.5
MHS model	m_1	[-]	0.743	0.529	0.687	0.525
	m_2	[-]	0.311	0.230	0.270	0.205
	δ_1	[-]	3.35E-02	1.97E-02	1.59E-02	1.33E-02
	τ	[s]	1.80E-06	1.34E-05	9.81E-06	1.02E-05
	G_∞	[MPa]	2815	4004	2576	3094
	G_0	[MPa]	3.36E-04	2.39E-02	4.74E-02	4.60E-02
	η_3	[MPa·s]	136	148200	19397	169374
R^2	@|G*|	[-]	0.999	0.999	0.999	0.999
	@θ	[-]	0.999	0.999	0.997	0.998

3.3 Shear fatigue life of bituminous mortars

Reduction of the complex shear modulus in shear fatigue test was considered by plotting the complex shear modulus versus the number of loading cycles. Figure 6 shows an example of the shear fatigue test result of a bituminous mortar in the strain-controlled mode. The complex shear modulus drops sharply at the initial stage of the test followed by a relatively linear low-rate decrease during the middle portion of the test. Afterwards, a sharp decrease of the complex shear modulus to a very low value occurs during the back portion of the test. Finally, the curve flattens towards the end of the test.

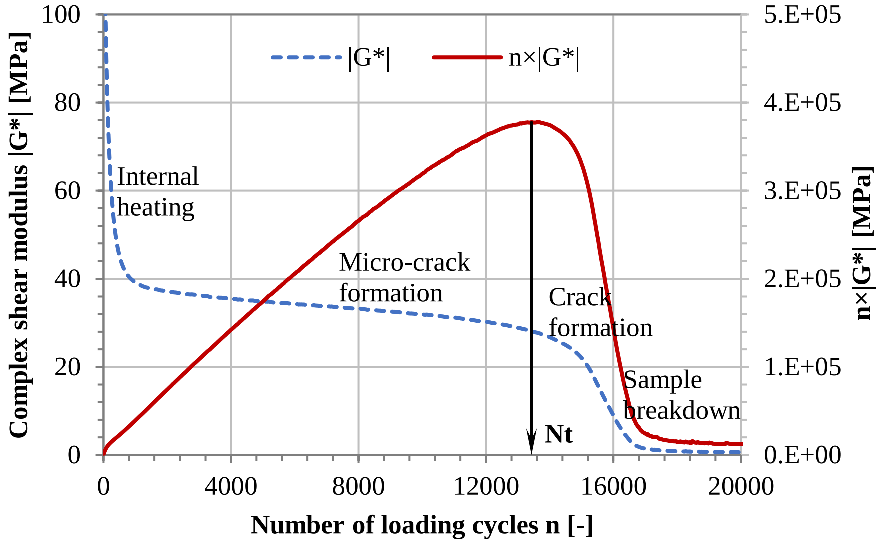

Figure 6: Example of the shear fatigue test result and the illustration of determining the shear fatigue life of a bituminous mortar specimen.

The failure criterion based on the 50% of initial stiffness (or modulus) method is commonly used in the fatigue tests of asphalt mixture under the strain-controlled mode. However, this criterion seems not able to capture the true fatigue failure of bituminous mortars, since 50% complex shear modulus reduction was often reached before the crack initiation in the bituminous mortars. The fatigue resistance evaluation method for asphaltic mixtures proposed by Rowe and Bouldin [32], which is based on energy ratio, was adopted to define the fatigue life of bituminous mortars in this research. In that method, the fatigue curves in the strain-controlled mode are subdivided into four regions: the initial specimen heating region, the micro-crack formation region, the crack formation and propagation region, and finally the specimen breakdown region (see Figure 6). The fatigue failure is defined as the point when the curve transitions from the micro-crack formation region to the crack formation and propagation region.

The transition point (Nt) is determined based upon evaluation of the product of stiffness and number of loading cycles. The meaning of the transition point can be explained mathematically using the Taylor's series expansion given in Equation 15 and 16. In the micro-crack formation region, the first differential (dE^*/dn) is a negative constant. The second differential (d^2E^*/dn^2) equals to zero. As cracks form and begin to propagate, the first differential (dE^*/dn) is still negative but increasing in magnitude. The second differential (d^2E^*/dn^2) becomes negative. So the product of stiffness and number of loading cycles reduces in the crack formation and propagation region. The resulting maximum indicates the transition point between micro-crack formation and crack formation. The transition point is a reasonably acceptable failure point, as reported by Kim et al. [33, 34].

$$E^* = E_0^* + n\frac{dE^*}{dn} + \frac{n^2}{2!}\frac{d^2E^*}{dn^2} + \frac{n^3}{3!}\frac{d^3E^*}{dn^3} + \cdots \tag{15}$$

$$E^*n = E_0^*n + n^2\frac{dE^*}{dn} + \frac{n^3}{2!}\frac{d^2E^*}{dn^2} + \frac{n^4}{3!}\frac{d^3E^*}{dn^3} + \cdots \tag{16}$$

Where E^* is stiffness or modulus; E_0^* is the initial stiffness or modulus; and n is number of loading cycles.

For each type of bituminous mortar, fatigue lives at nine strain levels were successfully acquired by means of analysing the transition points of cylindrical mortar specimens from the shear fatigue tests. The number of loading cycles to failure at applied strain levels was plotted on a log-log scale, as shown in Figure 7.

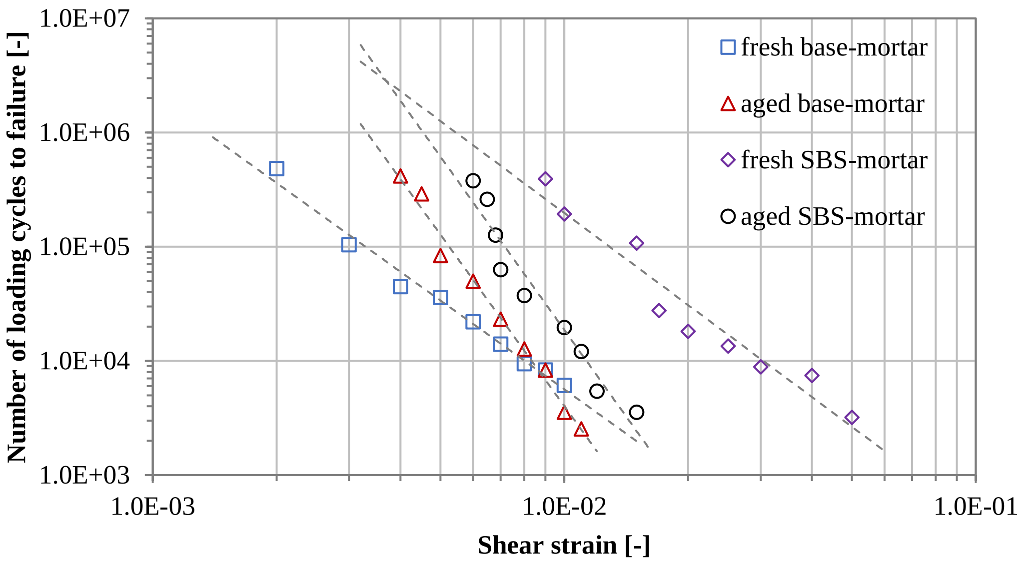

Figure 7: Fatigue relations between the number of loading cycles to failure and shear strain for fresh and aged bituminous mortars under the strain-controlled mode.

In Figure 7, the fresh mortar with base bitumen showed a longer fatigue life than its aged mortar at shear strain of higher than 8.6E-03. When shear strain is lower than 8.6E-03, its aged mortar had a longer fatigue life. The fresh mortar with SBS modified bitumen showed a longer fatigue life than its aged mortar at shear strain of higher than 3.7E-03. When shear strain is lower than 3.7E-03, its aged mortar had a longer fatigue life. This means ageing decreased the fatigue life of bituminous mortar at high strain levels, but increased its fatigue life at low strain levels. The fresh mortar with SBS modified bitumen showed higher fatigue life than fresh mortar with base bitumen. After ageing, the aged mortar with SBS modified bitumen still behaved better in fatigue resistance than the aged mortar with base bitumen. But the difference in fatigue lives between aged bituminous mortars is smaller than that between fresh bituminous mortars. Thus, it can be concluded that ageing resulted in more changes in the fatigue life of mortar with SBS modified bitumen than that of mortar with base bitumen.

Bituminous mortars exhibit viscoelastic behaviour, which leads to energy dissipation during cyclic loading. Dissipated energy is often used by researchers to explain fatigue damage development. Huurman et al. [14-15] proposed a mortar fatigue model based on the dissipated energy concept to explain the mortar fatigue behaviour. In their mortar fatigue model, the dissipated energy per cycle in the initial phase is considered to be indicative for the fatigue life. The dissipated energy per cycle in the initial phase can be determined by the total area of various stress-strain hysteresis loops. Equations 17 and 18 provides the mathematical expression of that mortar fatigue model.

$$N_f = (W_0/W_{initial})^n \tag{17}$$

$$W_{initial} = \int \sigma_{ij} d\varepsilon_{ij} \tag{18}$$

Where N_f is the number of loading cycles to failure; W_0 is the reference energy; $W_{initial}$ is the dissipated energy per cycle in initial phase; n is material constant; τ_{ij} is stress components; and ε_{ij} is strain components.

This mortar fatigue model will be used to interpret the stress and strain signals obtained from finite element modelling of PA wearing courses such that the mortar fatigue life can be predicted. For the shear fatigue test, the initial dissipated energy per cycle is equal to the area of the hysteresis loop obtained by plotting the shear stress against the shear strain. The initial dissipated energy per cycle for each mortar specimen measured in the shear fatigue test was calculated. In this research nine shear fatigue tests at different shear levels were performed for each type of bituminous mortar. The number of loading cycles to failure mentioned above was then plotted against the initial dissipated energy per cycle on a log-log scale. As indicated in Figure 8, the number of loading cycles to failure follows a linear relation with the initial dissipated energy per cycle on a log-log scale. Based on these data, the mortar parameters (reference energy W_0 and material constant n) were determined by the method of least square fitting. The obtained model parameters are given in Table 5. The values of coefficient of determination (R^2) indicate that the mortar fatigue model shows a good fit with the test results.

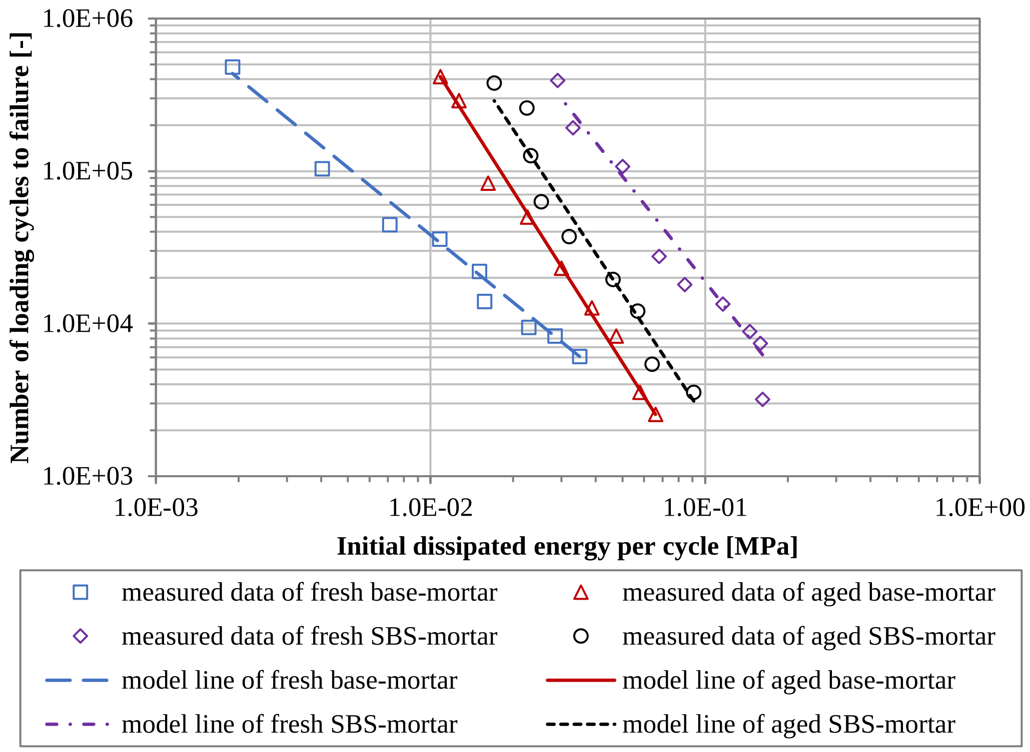

Figure 8: Relations between the number of loading cycles to failure and initial dissipated energy per cycle for fresh and aged bituminous mortars at 10 °C.

Table 5: Parameters of the mortar fatigue model based on the initial dissipated energy per cycle.

Mortar type		W_0 [MPa]	n [-]	R^2
Mortar with base bitumen	fresh	13.220	1.468	0.993
	aged	1.059	2.825	0.992
Mortar with SBS modified bitumen	fresh	7.322	2.293	0.975
	aged	1.771	2.709	0.954

3.4 Stress and strain simulation in PA models

The material responses of fresh and aged mortars with base bitumen were input into the PA 0/16 model for simulation. While the material responses of fresh and aged mortars with SBS modified bitumen were implemented in the simulation of PA 0/10 model. The shear stresses and strains that develops within the bituminous mortar in the model were output for analysis, as well as the shear stresses and strains. Figure 9 shows impressions of the distribution of maximum principal stress in the PA 0/16 and PA 0/10 models. Because ravelling of PA wearing course normally starts at the first stones on the surface, several critical locations within the bituminous mortar between the first stones on surface of the model were selected for analysis (see Figure 10). At all the selected locations, the bituminous mortar shows relatively higher levels of maximum principal stress or shear stress.

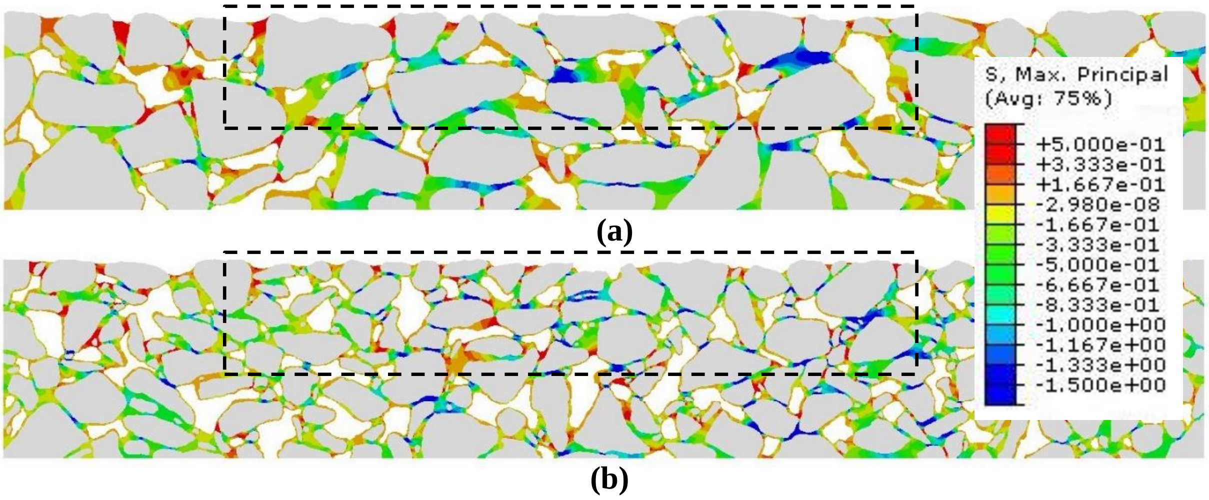

Figure 9: Impressions of the maximum principal stress distribution in the PA 0/16 model (a) and PA 0/10 model (b).

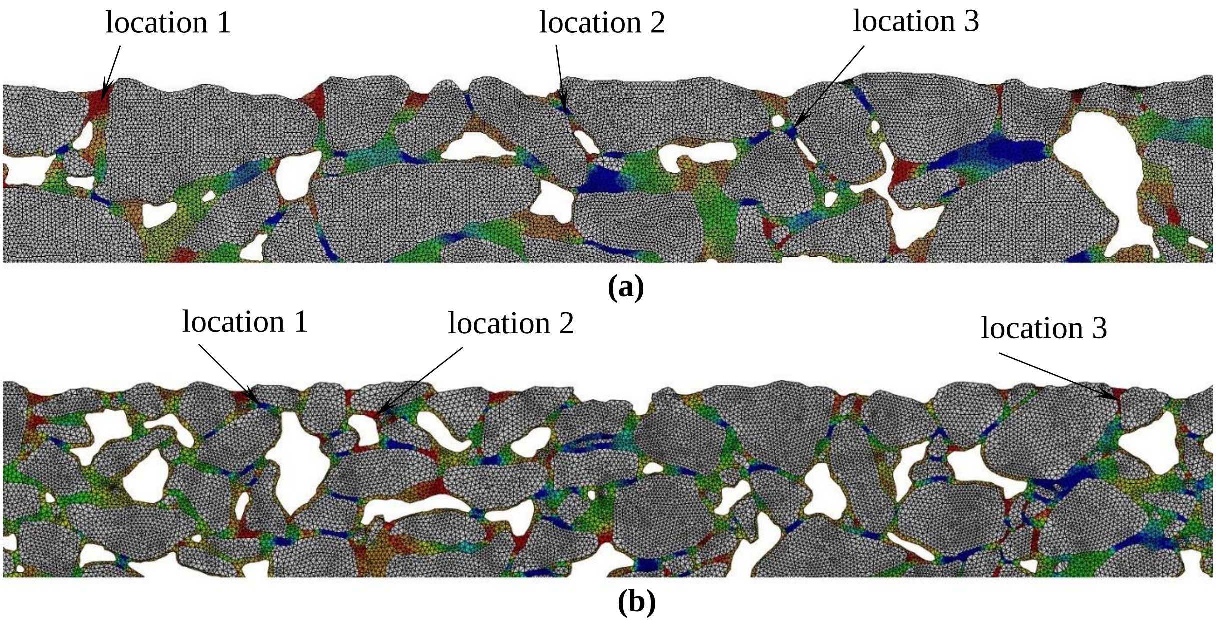

Figure 10: Selected locations for analysis from the PA 0/16 model (a) and PA 0/10 model (b).

Figure 11 presents an example of the hysteresis loops from shear stress and strain signals at location 1 in the PA 0/16 model. At this location, the shear stress changed slightly after ageing. While the shear strain had a large decrease after ageing. The initial dissipated energy per cycle at this location can be calculated from these hysteresis loops. For the fresh mortar with base bitumen it is 4.8E-04 MPa. For the aged mortar with base bitumen the value is 9.4E-05 MPa. Based to Equation 17 and Table 5, the fatigue lives of these mortars at location 1 can be calculated. The predicted fatigue lives of fresh and aged mortars at location 1 in PA 0/16 model are 3.3E+06 and 2.8E+11, respectively. The results of peak values of shear stress and strain from other locations in the PA 0/16 and 0/10 models are given in Table 6. The results of initial dissipated energy per cycle and predicted fatigue life that were calculated from the obtained shear stress and strain signals are presented as well.

As indicated in Table 6, aged mortars always showed higher values of predicted fatigue life than fresh mortars at the same location. This is consistent with the findings from shear fatigue tests that aged mortars had a longer fatigue life than fresh mortars at low levels of shear strains. Comparing the predicted fatigue lives between the PA 0/16 and 0/10 models, it can be found that bituminous mortar with SBS modified bitumen (in PA 0/16 model) had higher values of predicted fatigue life than bituminous mortar with base bitumen (in PA 0/10 model) before and after ageing. It indicates that the PA 0/10 wearing course with SBS modified bitumen had a better ravelling resistance than the PA 0/16 wearing course with base bitumen. But it should be noted that this advantage had weakened as the ageing of bituminous mortars.

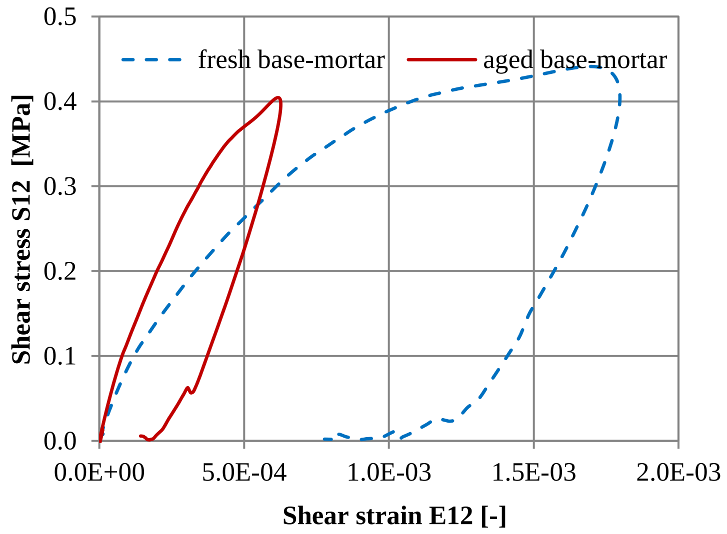

Figure 11: Example of the hysteresis loops from shear stress and strain signals at location 1 in the PA 0/16 model.

Table 6: Results from the stress and strain simulation in the PA models.

Model	Loca-tion	Mor-tar	Max. principal stress [MPa]	Max. principal strain [-]	Shear stress [MPa]	Shear strain [-]	Initial dissipated energy [MPa]	Predicted fatigue life [-]
PA 0/16	1	fresh	0.831	1.11E-03	0.441	1.80E-03	4.8E-04	3.3E+06
		aged	0.739	3.65E-04	0.404	6.27E-04	9.4E-05	2.8E+11
		Δ	-11%	-67.0%	-8.3%	-65.1%	--	--
	2	fresh	-2.191	1.37E-03	-0.777	-2.87E-03	1.5E-03	6.2E+05
		aged	-2.259	5.35E-04	-0.799	-1.12E-03	4.1E-04	4.4E+09
		Δ	3%	-60.9%	2.7%	-61.1%	--	--
	3	fresh	-1.594	2.12E-03	-1.473	-5.22E-03	4.9E-03	1.1E+05
		aged	-1.595	8.62E-04	-1.519	-2.10E-03	1.4E-03	1.4E+08
		Δ	0%	-59.4%	3.1%	-59.7%	--	--
PA 0/10	1	fresh	-1.405	1.77E-04	-0.255	-6.78E-04	1.1E-04	1.2E+11
		aged	-1.425	9.84E-05	-0.273	-3.94E-04	5.0E-05	2.1E+12
		Δ	1.4%	-44.5%	7.1%	-42.0%	--	--
	2	fresh	0.766	8.83E-04	-0.439	-1.48E-03	3.4E-04	8.6E+09
		aged	0.770	4.47E-04	-0.442	-7.56E-04	1.2E-04	2.0E+11
		Δ	0.5%	-49.3%	0.7%	-49.0%	--	--
	3	fresh	1.650	1.59E-03	-0.701	-2.42E-03	8.9E-04	9.5E+08
		aged	1.635	8.09E-04	-0.710	-1.24E-03	3.3E-04	1.3E+10
		Δ	-0.9%	-49.2%	1.3%	-48.5%	--	--

The shear stresses within bituminous mortars in the PA models changed slightly or nothing after ageing. However, the shear strains decreased significantly. For the PA 0/16 model, an average decrement of 62.0% was found in the shear strains after ageing. For the PA 0/10 model, an average decrement of 46.5% was found in the shear strains after ageing. Ageing resulted in stiffer bituminous mortars allowing less development of strain in the PA models. Table 6 also gives the results of peak values of maximum principal stress and strain from different locations of the PA models for comparison. The tendency of maximum principal stress is similar as that of shear stress. For the PA 0/16 model, an average decrement of 62.4% was found in the maximum principal strains after ageing. For the PA 0/10 model, an average decrement of 47.7% was found in the maximum principal strains after ageing. An interesting finding is that the decrements of the maximum principal strain and shear strain in the PA 0/16 model are approximately 15% higher than those in the PA 0/10 model. It indicates that ageing caused less change on the flexibility of bituminous mortar with SBS modified bitumen than that of bituminous mortar with base bitumen.

4. Conclusions

Based on the findings and analysis presented in this paper, the following conclusions can be drawn: (1) The rheological tests on the cylindrical mortar specimens provided very good result repeatability, as evidenced by the high anastomosis within the test results from different mortar specimens; (2) The master curves of complex shear modulus and phase angle of bituminous mortars were well described by the MHS model. Ageing had more influence on the complex shear modulus and phase angle of bituminous mortar with base bitumen compared with the bituminous mortar with SBS modified bitumen; (3) The fatigue failure of bituminous mortars in the strain-controlled shear fatigue test should be defined as the point when the fatigue curve transitions from the micro-crack formation region to the crack formation and propagation region, based upon evaluation of the product of stiffness and number of loading cycles. Ageing caused more changes on the fatigue resistance of the mortar with SBS modified bitumen than that of the mortar with base bitumen; (4) The bituminous mortars with similar complex shear modulus can have different performances of fatigue resistance; (5) The PA 0/10 wearing course with SBS mortar had a better ravelling resistance than the PA 0/16 wearing course with base mortar; (6) Ageing had more significant effect on the ravelling resistance of the PA 0/16 wearing course with base mortar than the PA 0/10 wearing course with SBS mortar.

This study has developed an efficient and reliable test protocol to quantify the ageing effects on the rheological characteristics of bituminous mortar. By following this protocol, future research can be conducted on measuring the properties of bituminous mortar under different ageing and rejuvenating conditions, based on which effective numerical models can be built to predict the performance of PA and evaluate the effectiveness of various preservative maintenance techniques for PA wearing courses.

Acknowledgements

The authors acknowledge the Department of Applied Biology and Chemical Technology in the Hong Kong Polytechnic University for providing support on the infrared spectrum tests required for this study.

References

[1] Highways Department, Road surface requirements for expressways and high speed roads, RD/GN/032, Research & Development Division, Highways Department, Hong Kong, 2007.

[2] S. Shimeno, A. Oi, T. Tanaka, Evaluation and further development of porous asphalt pavement with 10 years experience in Japanese expressways, Proceeding of the 11th International Conference on Asphalt Pavements, International Society for Asphalt Pavements, Lino Lakes, Minnesota, USA, 2010.

[3] S. Takahashi, Comprehensive study on the porous asphalt effects on expressways in Japan based on field data analysis in the last decade, Road Materials and Pavement Design 14 (2013) 139-255.

[4] L. Santha, A Comparison of modified open-graded friction courses to standard open-graded friction course, Publication FHWA-GA-97-9110, Georgia Department of Transportation, Georgia, 1997.

[5] G. Huber, Performance survey on open-graded friction course mixes, Synthesis of Highway Practice 284, Transportation Research Board, National Research Council, Washington, D.C., 2000.

[6] A.E. Alvarez, A.E. Martin, C.K. Estakhri, J.W. Button, C.J. Glover, S.H. Jung, Synthesis of current practice on the design, construction, and maintenance of porous friction courses, Publication FHWA/TX-06/0-5262-1, Texas Department of Transportation, Texas, 2006.

[7] L.A. Cooley, J.W. Brumfield, R.B. Mallick, W.S. Mogawer, M. Partl, L. Poulikakos, G. Hicks, Construction and maintenance practices for permeable friction courses, NCHRP Report 640, Transportation Research Board, National Research Council, Washington, D.C., 2009.

[8] J.H. Swart, Experience with porous asphalt in the Netherlands, Report W-DWW-97-058, Department of Civil Engineering Service, The Ministry of Infrastructure and the Environment, The Netherlands, 1997.

[9] Y. Zhang, Extending the lifespan of porous asphalt concrete, Ph.D. dissertation, Delft University of Technology, Delft, 2015.

[10] N. Verra, M. van den Bol, B. Gaarkeuken, The service life of porous asphalt, Report DWW-2003-066, Department of Civil Engineering Service, The Ministry of Infrastructure and the Environment, The Netherlands, 2003.

[11] E.R.P. Rutten, J.L.M. Voskuilen, F. Tolman, Does modified porous asphalt go longer? Report DWW-2002-13, Department of Civil Engineering Service, The Ministry of Infrastructure and the Environment, The Netherlands, 2002.

[12] J.K. Mohammad, V. Kyatham, Viscoelastic Behavior of Hydrated Lime-Modified Asphalt Matrix and Hot-Mix Asphalt under Moisture Damage Conditions, Journal of the Transportation Research Board 2370 (2008) 64–74.

[13] J.K. Mohammad, Z. You, V. Kyatham, On the Mechanical Modeling of Asphalt Matrix and Hot Mix Asphalt Mixtures. Proceeding of the Airfield and Highway Pavement 2008, Washington, D.C., USA, 2008.

[14] M. Huurman, L.T. Mo, M.F. Woldekidan, Unravelling Porous Asphalt Concrete towards a Mechanistic Material Design Tool, Road Materials and Pavement Design 11 (2010) 583–612.

[15] L.T. Mo, M. Huurman, M.F. Woldekidan, S.P. Wu, A.A.A. Molenaar, Investigation into Material Optimization and Development for Improved Ravelling Resistant Porous Asphalt Concrete, Materials and Design 31 (2010) 3194–3206.

[16] M.F. Woldekidan, M. Huurman, A.C. Pronk, A Modified HS Model: Numerical Application in Modeling the Response of Bituminous Materials, Finite Elements in Analysis and Design 53 (2012) 37–47.

[17] M.F. Woldekidan, M. Huurman, A.C. Pronk, Linear and Nonlinear Vicoelastic Analysis of Bituminous Mortar, Journal of the Transportation Research Board 2370 (2013) 53–62.

[18] B.S. Underwood, Y.R. Kim, Effect of Volumetric Factors on the Mechanical Behavior of Asphalt Fine Aggregate Matrix and the Relationship to Asphalt Mixture Properties, Construction and Building Materials 49 (2013) 672–681.

[19] P. Sousa, E. Kassem, E. Masad, D. Little, New Design Method of Fine Aggregates Mixtures and Automated Method for Analysis of Dynamic Mechanical Characterization Data, Construction and Building Materials 41 (2013) 216–223.

[20] Y. He, Z.A. Mohammad, D. Jones, J. Harvey, Proposing a solvent-free approach to evaluate the properties of blended binders in asphalt mixes containing high quantities of reclaimed asphalt pavement and Recycled Asphalt Shingles, Construction and Building Materials 114 (2016) 172–180.

[21] E.T. Hagos, The effect of aging on binder properties of porous asphalt concrete, Ph.D. dissertation, Delft University of Technology, Delft, The Netherlands, 2008.

[22] W. Van den Bergh, M.F.C. van de Ven, The influence of ageing on the fatigue and healing properties of bituminous mortars, Procedia – Social and Behavioral Sciences 53 (2012) 256–265.

[23] P.M. Muraya, Permanent deformation of asphalt mixtures, Ph.D. dissertation, Delft University of Technology, Delft, The Netherlands, 2007.

[24] Y. Zhang, M.F.C. van de Ven, A.A.A. Molenaar, M.F. Woldekidan, S. Wu, Mechanical properties of porous asphalt concrete with rejuvenators, Proceeding of the 9th International

Conference on the Bearing Capacity of Roads, Railways and Airfields, Trondheim, Norway, 2013.

[25] Y. Zhang, M.F.C. van de Ven, A.A.A. Molenaar, S. Wu, Preventive maintenance of porous asphalt concrete using surface treatment technology, Materials and Design 99 (2016) 262-272.

[26] M.F. Woldekidan, Response modelling of bitumen, bituminous mastic and mortar, Ph.D. dissertation, Delft University of Technology, Delft, 2011.

[27] M. De Beer, Measurement of tyre/pavement interface stresses under moving wheel loads, Research Report DPVT 224, Division of Road and Transport Technology, The Council for Scientific and Industrial Research, Pretora, 1994.

[28] M.F.C. van de Ven, J. Qiu, Y. Zhang, Increasing the functional service life of porous asphalt surfacings: development of test methods to study the effect of rejuvenating binders, Proceeding of the 15th International Flexible Pavements Conference of the Australian Asphalt Pavement Association, Queensland, 2013.

[29] J. Lamontagne, P. Dumas, V. Mouillet, J. Kister, Comparison by Fourier Transform Infrared (FTIR) spectroscopy of different ageing techniques: application to road bitumens, Fuel 80 (2001) 483–488.

[30] A.C. Pronk, The Huet-Sayegh model: a simple and excellent rheological model for master curves of asphaltic mixes, Proceeding of the R. Lyttom Symposium on Mechanics of Flexible Pavements, Louisiana, USA, 2005.

[31] C. Huet, Study of the viscoelastic behaviour of bituminous mixes by method of impedance, University of Paris, Paris, France, 2007.

[32] G.M. Rowe, M.G. Bouldin, Improved techniques to evaluate the fatigue resistance of asphaltic mixes, Proceeding of the 2nd Euraphalt and Eurobitume Congress, Barcelona, Spain, 2000.

[33] Y.R. Kim, D.N. Little, I. Song, Effect of mineral fillers on fatigue resistance and fundamental material characteristics: mechanistic evaluation, Journal of the Transportation Research Board 1832 (2003) 1–8.

[34] Y.R. Kim, D.N. Little, Development of specification-type tests to assess the impact of fine aggregate and mineral filler on fatigue damage, Publication FHWA/TX-05/0-1707-10, Texas Department of Transportation and Federal Highway Administration of U.S. Department of Transportation, 2005.